

Lab Report

Rastertunnelmikroskopie

Moritz Dahm, Ole Kleinjung, Felix Möckel

Tutor: Bharti Mahendru

Fortgeschrittenenpraktikum, WS 2024/25
Berlin, 20.01.2024

Freie Universität Berlin
Fachbereich Physik

Contents

1	Introduction	3
2	Theory	3
2.1	Quantum tunneling	3
2.2	Theory of STM	3
2.3	Graphite structure	4
2.4	Piezoelectric Effect	5
2.4.1	Piezoelectric Creep	5
3	Setup and working principle	5
3.1	PID-Controls	6
4	Procedure	6
5	Results	7
5.1	Steps on Graphite surface	7
5.2	Scanning settings	9
5.3	Planar distance between closest neighbors of graphite	10
5.3.1	Real space	10
5.3.2	Reciprocal space	12
6	Discussion	13
6.1	Step Heights in Graphite	13
6.2	Scanning settings	14
6.3	Planar distance between closest neighbors of graphite	14
7	Quellen	15

1 Introduction

Scanning tunneling microscopy (STM) provides the ability to image and resolve surfaces down to the scale of atomic distances, enabling non-destructive material analysis. It utilizes the tunneling current that arises when a metallic tip is brought into close proximity to the surface and a voltage is applied between the tip and the sample. This experiment serves as an introduction to the application of scanning tunneling microscopy, by investigating the surface of graphite and determining its lattice constants.

2 Theory

2.1 Quantum tunneling

The following subsection is based on source [3].

The tunneling effect in quantum mechanics arises from the fact that particles can have a probability of being present in regions that would classically be "forbidden" due to insufficient energy. This leads to the phenomenon where electrons incident on a potential barrier can be transmitted, even if the energy of the barrier is greater than that of the electron. In the following, this scattering problem will be briefly solved using the Schrödinger equation:

$$\left(-\frac{\hbar^2}{2m}\partial_x^2 + V(x)\right)\psi(x) = E\psi(x) \quad (1)$$

Let us consider a box potential:

$$V(x) = \begin{cases} V_0, & \text{if } 0 < x < a. \\ 0, & \text{otherwise.} \end{cases} \quad (2)$$

such that the energy of the electron satisfies $0 < E_0 < V_0$. Representing the energy of the electron as $E_0 = \frac{\hbar^2 k^2}{2m}$ and $E_0 - V_0 = -\frac{\hbar^2 \kappa^2}{2m}$ for $0 < x < a$, the solution to the Schrödinger equation is given by:

$$\psi(x) = \begin{cases} e^{ikx} + re^{-ikx}, & x < 0 \\ Ae^{\kappa x} + Be^{-\kappa x}, & 0 < x < a \\ te^{ikx}, & x > a \end{cases} \quad (3)$$

where the amplitude for the incident electron is set to 1. The transmission coefficient T in this case is given by $T = |t|^2$. Using the boundary conditions of the wave function at positions 0 and a , the transmission probability is derived as:

$$\frac{1}{T} = 1 + \frac{V_0^2}{4E_0(V_0 - E_0)} \sinh^2(a\kappa) \quad (4)$$

From the sinh function, which can be expressed in terms of exponential functions, it can be seen that the tunneling probability, and thus the resulting tunneling current in scanning tunneling microscopy, decreases exponentially with the width of the potential barrier.

2.2 Theory of STM

The content of the following subsection is based on the conversation with the tutor before the experiment.

The scanning tunneling microscope uses the tunneling effect to examine the surface of a conducting material, such as graphite. A metal tip is brought close to the surface of the material, which leads to electrons tunneling from the tip to the material and from the material to the tip. This process is described in subsection 2.1, where the potential is given by the air between tip and surface. Because the electrons tunnel both ways, there would be no measurable current. This can also be explained in another way: As the tip and the material are in equilibrium, the Fermi levels have to be aligned. Therefore there are no unoccupied states in the tip or the sample, which an electron could occupy, as the unoccupied states have higher energy than the Fermi levels. To measure a tunneling current one needs to apply a bias voltage V_{bias} , meaning a difference in electric potential, to the material, which raises its Fermi level by eV_{bias} , where e is the elementary charge. The electrons now have enough energy to tunnel from the material to the tip, as the states in the tip with energy higher than its Fermi level are unoccupied. This leads to a measurable current from material to tip, which depends, among other things, exponentially on the distance between tip and material.

For an electron to tunnel from surface to tip it is necessary that the electron is first emitted out of the solid, which requires energy. The energy required to take an electron out of a solid is called the work function ϕ . It depends on the Fermi level of the solid and is given by the difference of the vacuum energy to the Fermi level

$\phi = E_{vac} - E_F$. Comparing this to $\kappa = \frac{\sqrt{2m(V_0 - E_0)}}{\hbar}$ from section 2.1 yields $\kappa \propto \sqrt{\phi}$ if $V_0 = E_{vac}$ and $E_0 = E_F$, which results in an exponential decay of the transmission probability and therefore the tunneling current with respect to the squareroot of the work function. In total the proportionality of the tunneling current I_t is given by

$$I_t \propto V_{bias} \exp(-a\sqrt{\phi}) \quad (5)$$

2.3 Graphite structure

Solids consist of atoms or molecules that form bonds due to their interactions and arrange themselves into a crystal structure. Depending on the type of atoms involved and the resulting forces, different crystal structures emerge⁴. These structures can be described using the 14 different Bravais lattices, each of which can contain a basis at every lattice point, potentially consisting of multiple atoms. The conventional unit cell of the real space lattice is called the Wigner-Seitz cell. By applying a Fourier transformation, a reciprocal lattice can be introduced. The Wigner-Seitz cell of the reciprocal lattice is known as the Brillouin zone⁴.

Graphite consists of carbon atoms (C). Two of the six electrons of C occupy the 1s level, two occupy the 2s level, and the remaining two electrons are in the 2p_x and 2p_y levels. Only the electrons in the second shell play a role in the chemical properties. The probability distribution of electrons in the s-level is spherical (isotropic), while in the p-levels, it is anisotropic, resulting in dumbbell-shaped distributions⁴.

The four electrons from the s- and p-levels can hybridize. If all four electrons participate, an sp³ orbital forms, leading to the diamond structure. However, if only three electrons are involved, sp² orbitals form, giving rise to the graphite structure⁵. These sp² orbitals arrange themselves within a plane (surface), making the structure effectively two-dimensional; the remaining p-orbital is perpendicular to this plane. The orbitals within the plane have equal angles of 120° to each other, resembling the configuration shown in Fig. 1. The

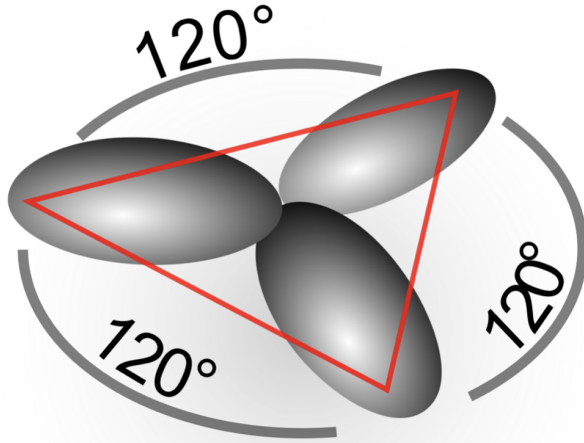


Figure 1: Hybridized sp²-orbital⁶

participating sp² atoms form covalent bonds with each other, resulting in a trigonal structure within the plane. The remaining p-orbitals interact with one another, but with significantly lower binding energies. As a result, a double bond is formed overall.

The successive layers are arranged according to the ABAB stacking sequence (as opposed to the ABC sequence). Due to this ABAB arrangement, some carbon atoms are positioned directly above one another. This implies that at these positions the probability of tunneling downwards is significantly greater than tunneling upwards. If tunneling occurs, it is more likely to happen downwards than upwards, which is why these atoms are ultimately not visible in the STM image. The measured STM structure is therefore not exactly the graphite structure, but it can be quickly arrived at by conversion (see section 5.3).

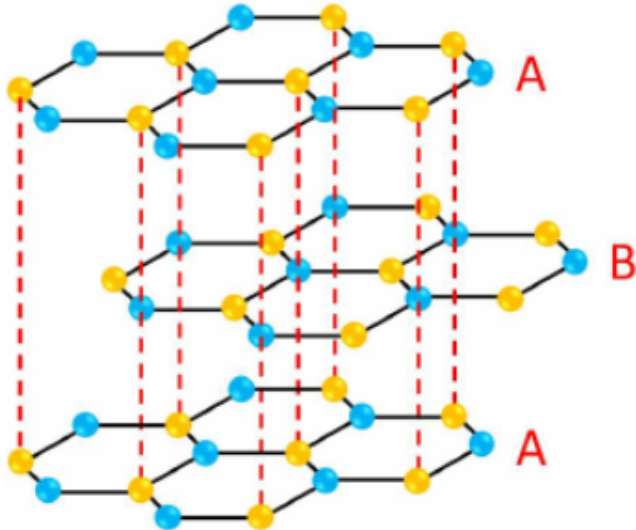


Figure 2: ABAB-stacking of honeycomb lattice of graphite [13]

2.4 Piezoelectric Effect

The piezoelectric effect describes the generation of a voltage in a material (molecule, solid, etc.) due to the application of mechanical pressure. Because of the inherent polarity in the material, compressing it creates a voltage between two opposite sides. However, the direction of the voltage does not always align with the direction of the applied mechanical pressure, as it varies depending on the material. The magnitude of the voltage is directly proportional to the applied pressure. The reverse effect is also possible: when an electrical voltage is applied, the material undergoes deformation (inverse piezoelectric effect). This property allows an STM to be moved with high precision using electrical signals².

2.4.1 Piezoelectric Creep

The piezoelectric effect induces a rapid response to voltage changes, initiating movement immediately. However, a phenomenon known as piezoelectric creep also occurs: there is a small delay before the movement begins, and when the voltage change stops, the piezoelectric actuator does not halt its motion immediately but continues to expand or contract slightly⁹. This behavior arises because piezoelectric materials possess an asymmetric charge distribution, leading to the formation of electric dipoles. These dipoles form local domains, which contribute to an overall dipole moment. When an electric field is applied, the domains expand—but the reorientation of dipoles takes some time as the system seeks a new equilibrium state. The direction of piezoelectric creep always follows the direction dictated by the change in the applied field⁹. The amount of creep occurring over a given time can even be mathematically described. However, a detailed discussion of this will not be provided here.

3 Setup and working principle

The schematic structure of a STM is shown in Figure 2. For understanding the principle of an STM, the right part of the image is particularly important. As illustrated, a tip connected to a component equipped with piezoelectric elements is brought close to the sample. This piezoelectric component is typically tubular, allowing movement of the tip in all three spatial directions via the inverse piezoelectric effect. The tip itself is made of a conductive material. There also is a bias voltage applied to the material.

Once the tip has been positioned in an initial state where a baseline tunneling current can be measured, there are two main methods for scanning the sample in the xy-plane. Either the tip's height (z-coordinate) is kept constant during scanning, or it is actively adjusted. If the tip moves at a constant height above the sample, either the tunneling current or the applied voltage is held constant. When the surface topography changes, the other parameter must be adjusted accordingly to maintain this condition, allowing detection of surface features. For example, if the tunneling current is kept constant and the tip encounters a raised area on the sample, the applied voltage must decrease because the tunneling probability increases. If both the voltage and the tunneling current are kept constant, the tip must always remain at the same distance from the sample. Since small variations in the tunneling current would require spatial adjustments, the control signal (z-coordinate adjustment) and the current signal are interconnected. The surface of the sample can then be reconstructed

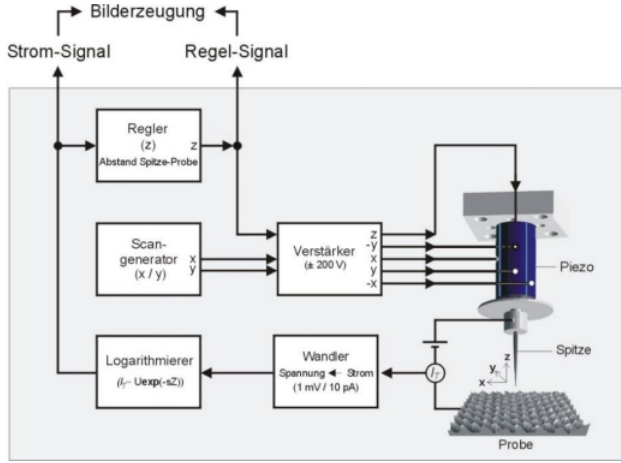


Figure 3: Schematic structure of an STM¹

based on the tip's movement. For this experiment the tunneling current and the bias voltage, and thus the distance from tip to surface, is held constant.

3.1 PID-Controls

In constant current mode, the tip keeps the tunneling current constant by measuring the tunneling current and moving away from or towards the surface when the measured current changes. Therefore, there need to be controls which dictate the tip how to optimally reach the desired current, if it is different from the measured one. Those controls are called PID, where P stands for proportional, I for integral, and D for differential. The proportional control corresponds to how big the difference between the measured and the wanted current is and thus produces a change in the measured current proportional to this difference. To explain the integral and differential control, it is best to imagine the measured current as a function of time, where the desired current would be a constant function. The integral control corresponds to the difference between the area under the curve of the measured current and the area under the constant function and thus to the total past error of the measured current. For example, if the measured current is consistently higher or lower than the desired one, the integral control can fix it. Finally, the differential control corresponds to the derivative of the measured current and dictates how fast the measured current should be changed towards the desired value. A value can be assigned to each one of the controls P, I and D, which determines how much each control is taken into account for the repositioning of the tip. How close those given values are to the theoretically optimal values defines how precise the measured current matches the desired one[12].

4 Procedure

The execution of this experiment begins with the preparation of the graphite . To create a surface as free from large defects as possible, the graphite plate is covered with a strip of adhesive tape and then peeled off along with the top graphite layers. This not only creates a surface where the steps are limited to a few atomic layers but also ensures that the graphite layer, which has been exposed to air for a long time, is removed. When stored in air, oxidation can occur, which is not desired in this experiment. The prepared plate is then placed in the scanning tunneling microscope (STM), and the tip of the microscope is first positioned using a hand screw and then adjusted with a stepper motor to the desired position. Various measurements are then carried out on the computer using the STM with the following settings:

- $V_{bias} = 100\text{mV}$
- P-gain=0.12
- scan speed=2.959 lines per second

The first approximately 40 measurements are used for step evaluation. After each completed measurement, the measurement area is changed so that no step is recorded twice. After this measurement series, a smooth and as flat as possible area on the graphite is sought by scanning different measurement regions. Once a suitable area is found the bias voltage, P-gain and measurement speed are varied, and images are taken for different settings. The final task is to capture images of the surface with atomic resolution. Since this was not successful, data provided by the experiment supervisor is analyzed instead.

5 Results

5.1 Steps on Graphite surface

To analyze the occurring step heights in graphite, the recorded surface images were evaluated using the WSxM software. For this purpose, the images are opened in the program with the 'Flatten' setting, and the steps are processed using the plane correction so that the two levels of the step are as uniform as possible, as shown in Figure 4. The step can then be plotted using the profile function. The obtained data can be fitted using a step function.

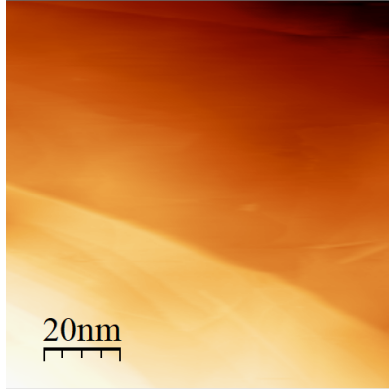


Figure 4: Example of an analyzed step in WSxM software.

Settings: $V_{bias} = 100\text{mV}$, P-gain=0.12, scan speed=2.959 lines per second

The procedure for determining the step height, including errors, is explained using an example (see Fig. 5). After the height values of a step are plotted, the best-fitting step function is added to the plot by eye as shown in the mentioned figure. Here, the height of the function/step, the position, and the offset can be manually adjusted. To determine the errors, the two step functions are found that have the greatest height difference from the original but still reasonably fit the data. The larger of these height differences is then taken as the error of the height in both directions. The recorded values are presented in Table 1.

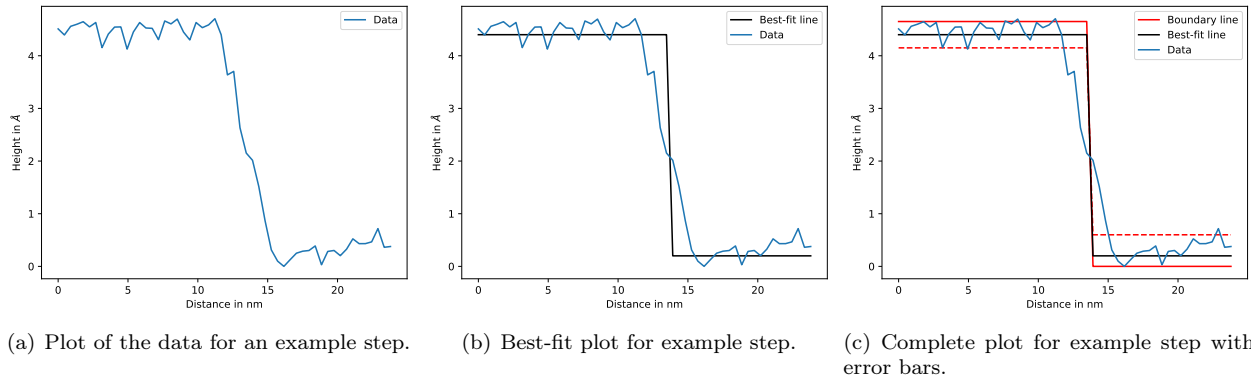


Figure 5: Procedure to analyze step heights.

This data is shown in Figure 6 in a histogram. The histogram has a bin width of 0.4\AA .

Table 1: Stepheights for different steps of graphite

Step	Height in Å
1	1.1 ± 0.2
2	1.45 ± 0.3
3	4.2 ± 0.37
4	1.21 ± 0.17
5	2.5 ± 0.35
6	1.0 ± 0.22
7	1.65 ± 0.28
8	2.0 ± 0.45
9	1.86 ± 0.2
10	2.2 ± 0.24
11	5.9 ± 0.65
12	4.3 ± 0.45
13	1.5 ± 0.33
14	3.0 ± 0.38
15	6.6 ± 0.54
16	4.0 ± 0.2
17	2.0 ± 0.18
18	1.15 ± 0.18
19	6.5 ± 1.3
20	5.0 ± 0.38
21	1.1 ± 0.1
22	2.2 ± 0.28
23	4.95 ± 0.28
24	4.95 ± 0.8

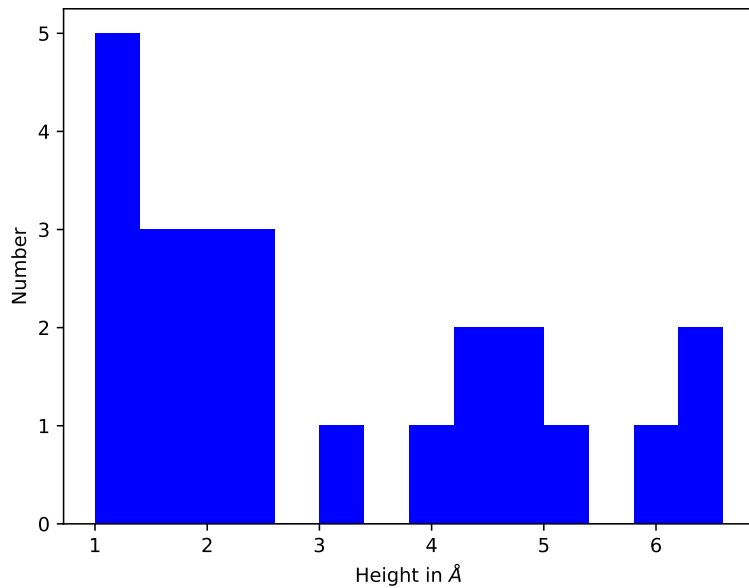


Figure 6: Histogram of the step heights in graphite

5.2 Scanning settings

In Fig. 7 there are two images taken with the STM. The left subfigure (a) has a P-gain of 0.12, the right subfigure (b) has a P-gain of 0.5. Comparing the two pictures, one can see that the higher P-gain leads to a grainy image, while the lower P-gain image is clearer and easier to analyze. The high P-gain leads to the PID-control overestimating the difference between the measured tunneling current and the desired one and overcorrects this difference by moving the tip too far away or towards the surface. This overcorrection happens over and over again, such that the resulting image appears grainy and unsMOOTH. This is amplified by the fact that the I-gain is fixed as half of the P-gain value. A bigger P-gain therefore yields a bigger I-gain.

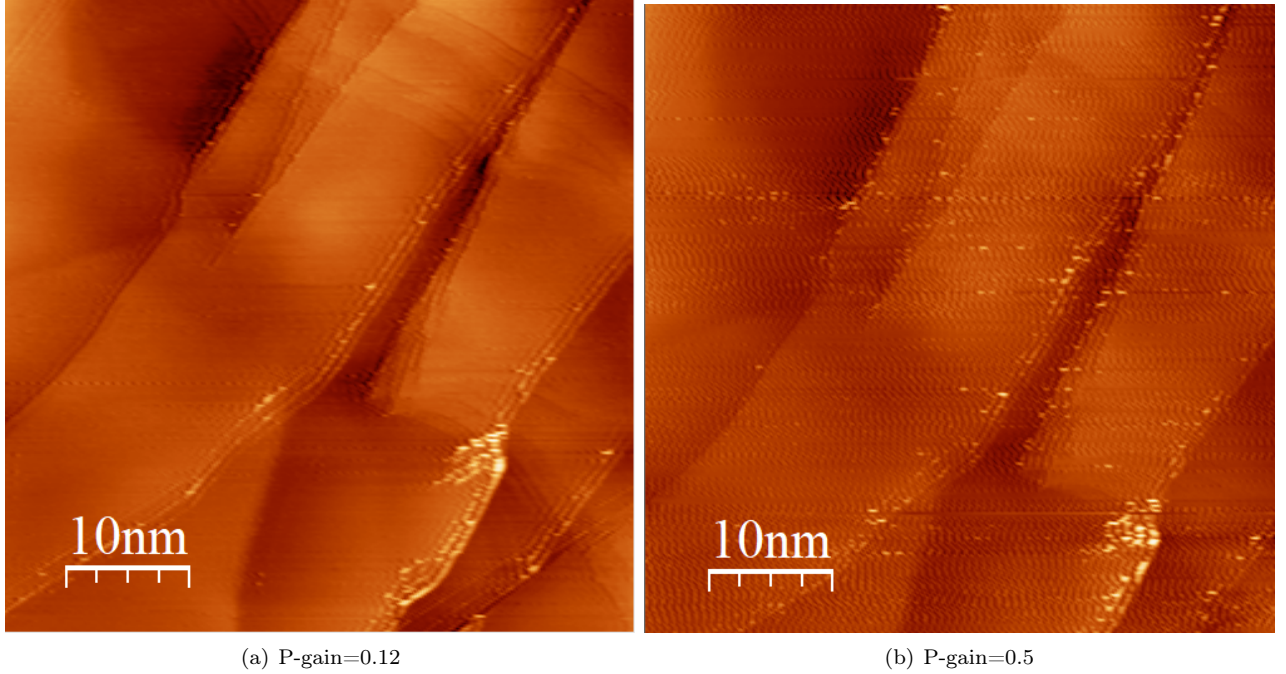


Figure 7: Comparison of two scans with different P-gain values. Both scans have $V_{bias} = 100\text{mV}$ and a scan speed of 2.959 lines per second

In Fig. 8 there are three images taken with different scan-speed settings. For subfigure (a) the STM scanned 2.959 lines per second, for subfigure (b) 4.65 lines per second and for subfigure (c) 8.138 lines per second. The different colors, coming from color adjusting mid measurement, should not distract from the difference in these pictures, which is the resolution. While big edges and steps are still recognizable with a high scan speed, the small details are lost. This is explainable by considering that the higher scan speed leads to less time for the setup to adjust to changes in the measured tunneling current. Little changes in the surface topography of the surface can therefore not be accounted for by the scan. In Fig. 9 there are three images taken with different bias

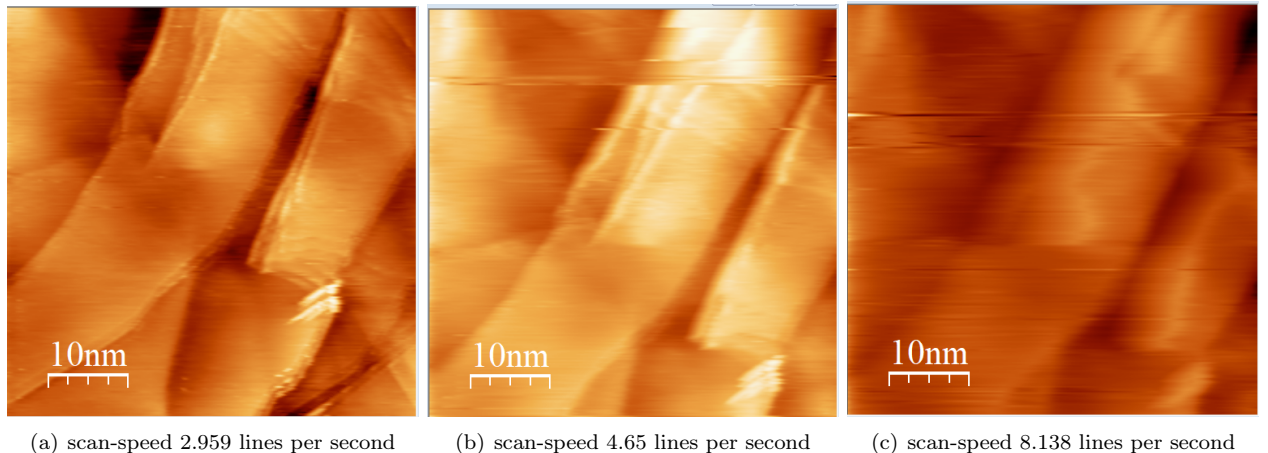


Figure 8: Comparison of three scans with different scan-speed values. All scans have $V_{bias} = 100\text{mV}$ and a P-gain of 0.12

voltages. For subfigure (a) the bias voltage is 30 mV, for subfigure (b) 60 mV and for subfigure (c) the upper half is with 100 mV and the lower half 30 mV. For (c) the bias voltage was changed mid-measurement. As Eq. (5) shows, the tunneling current is proportional to the bias voltage. A higher bias voltage consequently leads to the distance from tip to surface being higher (in constant current mode). But theoretically, the measured topography should not change for different bias voltages, as the change in distance from tip to surface needed to change the tunneling current is the same for different bias voltages, if they are constant during the measurement. This prediction is confirmed by the pictures in Fig. 9, as there are not really any differences to be seen. The subfigure (c) is slightly shifted to the top, which is why it looks kind of different.

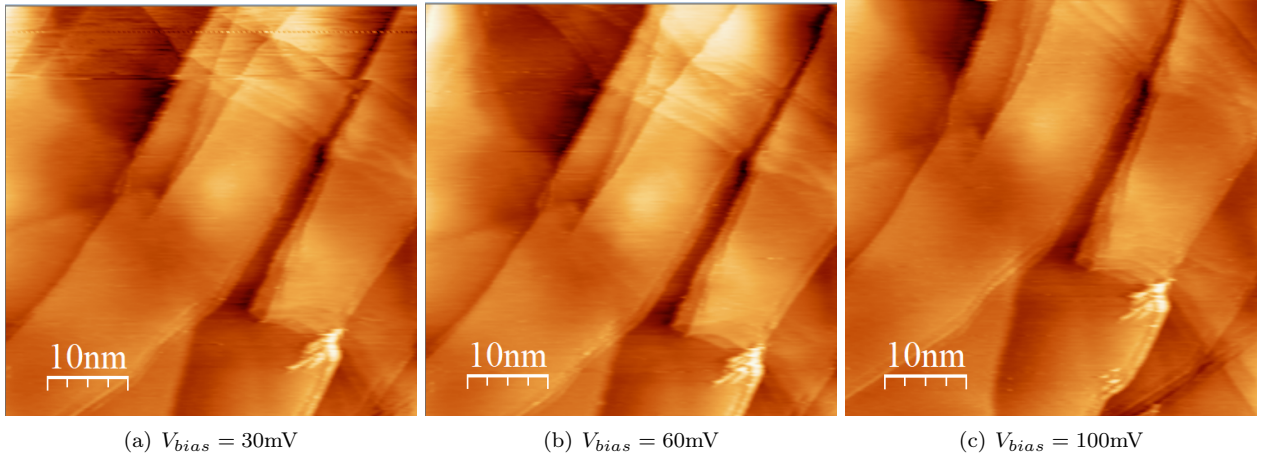


Figure 9: Comparison of three scans with different bias voltages. The images (a) and (b) were measured with a P-gain of 0.12 and a scan speed of 2.959, (c) was measured with P-gain of 0.7 and a scan speed of 6.51 lines per second.

5.3 Planar distance between closest neighbors of graphite

5.3.1 Real space

The atomic lattice structure of graphite can be resolved using the STM. Due to the fact that some atoms lie directly on top of each other, they are ultimately not visible in the STM image (see theory), so that a hexagonal structure can be seen whose atomic distances do not correspond to the actual atomic distances in graphite. The actual atomic spacing can be obtained by carrying out simple trigonometric considerations: In Fig. 10 shows a graphite plane. The atoms that are visible through the STM are shown in brown, while the atoms shown in gray are not visible. u and v are basis vectors of the hexagonal lattice. The distance $a = 142\text{ pm}$ is the actual atom distance, while the $b = 246\text{ pm}$ can be seen in the STM. With the structure shown in Fig. 10, the following equation can be established:

$$\cos(\gamma) = \frac{b/2}{a} \quad (6)$$

Here, $\gamma = (120 - 90)^\circ = 30^\circ$. It therefore follows that the desired atomic distance a can be determined by substituting the distance b in the following way:

$$a = \frac{b}{2 \cdot \cos(\pi/6)} \quad (7)$$

This will now be used to determine the atomic spacing of graphite. In Fig. 11 you can see an exemplary STM image that shows the hexagonal structure described.

This is now evaluated for all 3 occurring symmetry directions, indicated by the light blue line, and the two black lines in Fig. 11. As many atoms as possible are included, i.e. the N -fold atomic distance is measured in order to subsequently obtain a more precise determination of a single atomic distance b (divide by N). Fig. 12 shows an example of the evaluation process for one direction.

To determine the error of the result, the Full Width at Half Maximum (FWHM) of the two peaks used for evaluation is determined. The larger of the two FWHMs is divided by N and gives the error in both directions. This is justified because using N peaks significantly reduces the uncertainty. The results are intermediate results and the errors are therefore commercially rounded to two significant digits. The results for the three directions

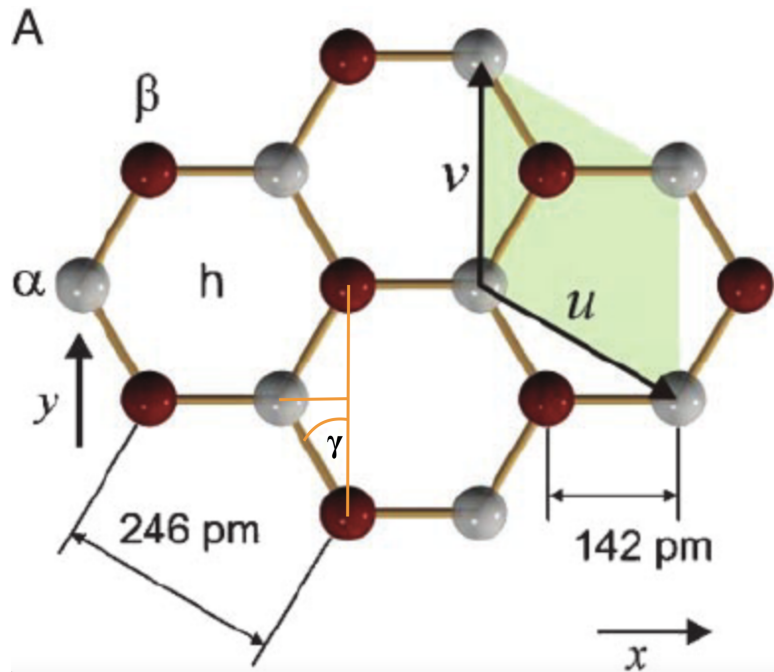


Figure 10: Structure of Graphite [11]

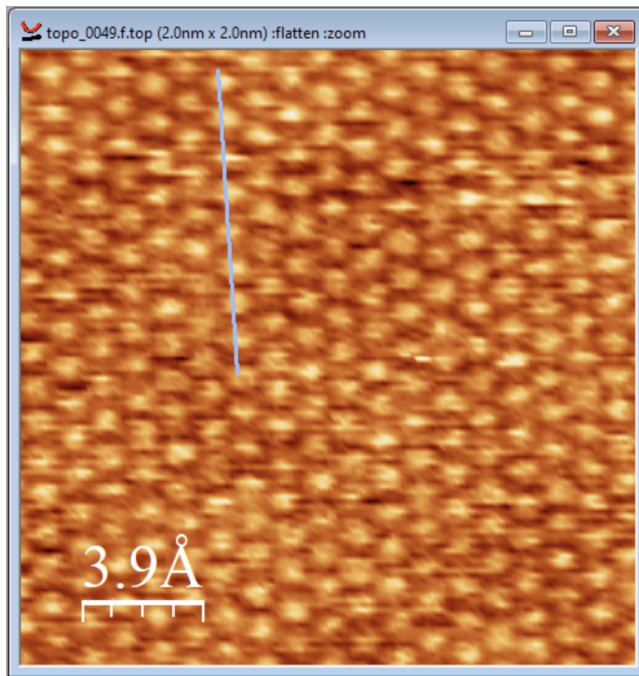


Figure 11: Example image of the STM of atomic resolution

are:

$$\begin{aligned} b_1 &= (1.06 \pm 0.11) \text{ \AA} \\ b_2 &= (1.15 \pm 0.11) \text{ \AA} \\ b_3 &= (1.18 \pm 0.20) \text{ \AA} \end{aligned} \quad (8)$$

The mean value can be taken from this (with the corresponding propagated error, largest error divided by $\sqrt{3}$):

$$b_{\text{exp}} = (1.13 \pm 0.12) \text{ \AA} \quad (9)$$

Finally, this result can be converted to obtain the required lattice constant a . Equation 7 is used for this. The result is final:

$$a_{\text{exp}} = (0.7 \pm 0.1) \text{ \AA} \quad (10)$$

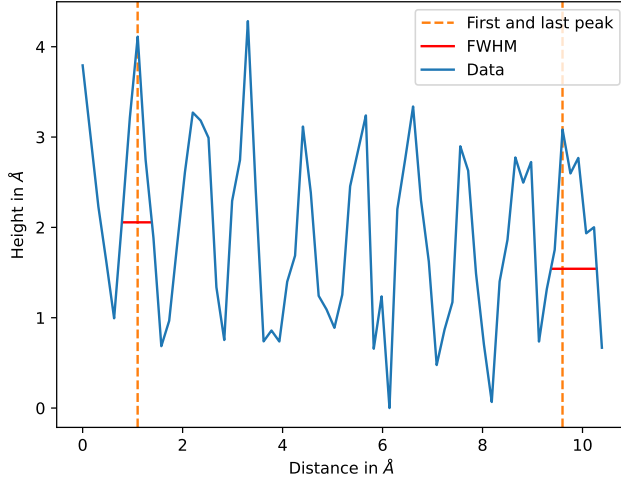


Figure 12: Example analysis for the lattice constant

5.3.2 Reciprocal space

To obtain the lattice constant from a reciprocal length in the reciprocal space (Fourier-transform of real space image), the value has to be converted into a length in real space. As the STM-image of graphite is not the honeycomb structure (not Bravais) of graphene but rather a hexagonal lattice (Bravais), one can easily find a basis $\{\vec{a}_1, \vec{a}_2\}$ for this lattice. In Fig. 13 there are two possible lattice vectors forming a basis, which are given by:

$$\vec{a}_1 = a(1, 0)^T \quad \vec{a}_2 = \frac{a}{2}(-1, \sqrt{3})^T \quad |\vec{a}_1| = |\vec{a}_2| = a \quad (11)$$

where the value $\sqrt{3}/2 = \sin(\pi/3)$ can be calculated by simple trigonometry. The reciprocal basis vectors \vec{g}_i fulfill the condition

$$\vec{a}_i \cdot \vec{g}_j = 2\pi\delta_{ij} \quad (12)$$

which results in 4 equations for 4 variables, which then give the reciprocal basis vectors:

$$\vec{g}_1 = \frac{2\pi}{\sqrt{3}a}(\sqrt{3}, 1)^T \quad \vec{g}_2 = \frac{4\pi}{\sqrt{3}a}(0, 1)^T \quad |\vec{g}_1| = |\vec{g}_2| = \frac{4\pi}{\sqrt{3}a} \quad (13)$$

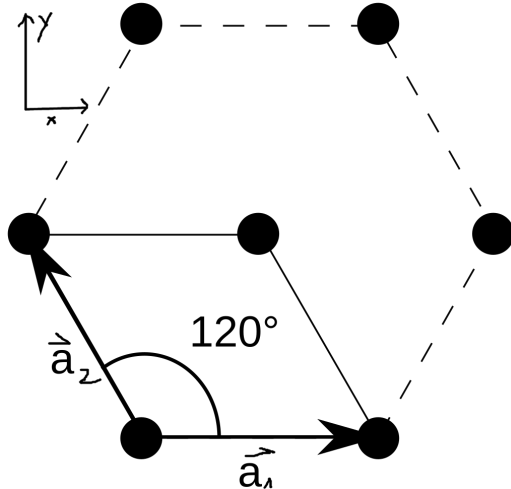


Figure 13: Basis vectors in hexagonal lattice (real space). [10]

This is to be used to confirm that a can also be determined via a Fourier transformation of the STM image in real space. The reciprocal lattice is therefore analyzed. In Fig. 14 shows a Fourier-transformed STM image that can be used for evaluation. This is analyzed similarly to the procedure in real space: The distance of the center point to neighboring points is taken in all 3 directions. The error is also determined in the same way as

above. As the option 1/wavelength was selected in the program for the Fourier transformation, the result must be multiplied by 2π in order to obtain the reciprocal grid vector. This results in the following three values for g :

$$\begin{aligned} g_1 &= (6.19 \pm 0.72) \text{ 1/\AA} \\ g_2 &= (6.47 \pm 0.63) \text{ 1/\AA} \\ g_3 &= (5.68 \pm 0.69) \text{ 1/\AA} \end{aligned} \quad (14)$$

If the mean value is determined from this again, b can then be determined again using equation (13). The final result here is when Gaussian error propagation is used again:

$$b_{\text{exp},2} = (1.19 \pm 0.28) \text{ \AA} \quad (15)$$

And finally, this results in the lattice constant:

$$a_{\text{exp},2} = (0.7 \pm 0.2) \text{ \AA} \quad (16)$$

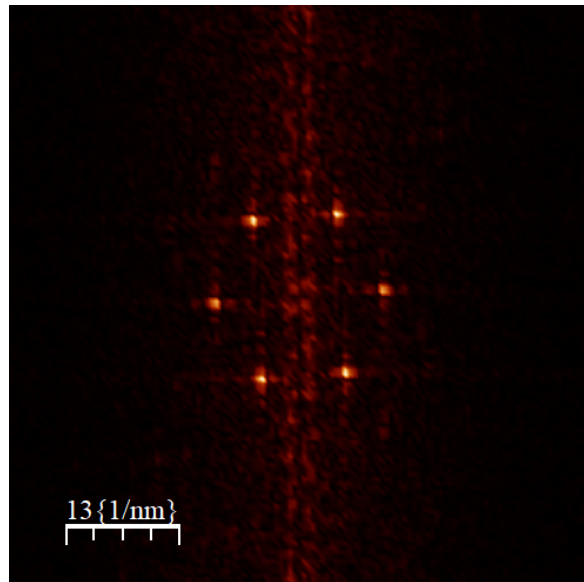


Figure 14: Fourier transform of STM image (Fig. 11)

6 Discussion

6.1 Step Heights in Graphite

A problem that occurred while evaluating the data on step height was that some data were presumably damaged during transport or recorded under incorrect settings. At least a significant portion of the data was unusable, as the images appeared similar to those shown in Figure 14. As a result, in order to evaluate a meaningful amount of data, steps had to be analyzed that could not be completely cleaned of disturbances even with plane correction. This contributed to the larger errors in Table 1. Nevertheless, an effort was made to examine as many meaningful steps as possible, which is also evident in the histogram 6. Comparing the values from table 1 with the theoretical value for the distance between levels in graphite, which is given by 3.35 \AA [1], one can see that the values do not match. Especially, the number of steps which have a lower value than the literature value is noticeable. Those values thus either come from height differences which do not correspond to a full distance of graphite layers or are not measured correctly. The incorrect measurement can result from the calibration of the piezos, because those could not be checked prior to the experiment. Additionally, the plane correction from the used program seemed to sometimes mess up the heights. As it is not exactly known how the plane correction works, the problem could be coming from there. Nevertheless, there are some values which could correspond to the literature value: Step 14 in table 1 is in range of the literature value with its error. Step 15 and 19 in table 1 are in range of two times the literature value and could correspond to a two level step. But as there are only 3 out of 24 measured steps which agree with the literature value, this measurement cannot be seen as successful.

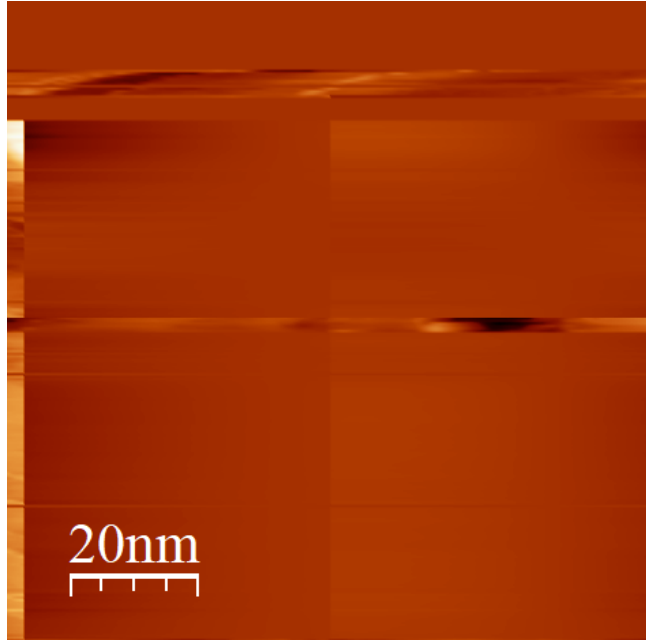


Figure 15: Example of unusable data

6.2 Scanning settings

It could be determined that changing the scanning settings regarding scan speed and proportional control of the STM changes the resulting image. Furthermore, the settings used for the measurement of the step heights (see section 4) seem to be ideal, as a higher P-gain leads to a grainy image and a higher scan speed, which would make the measurement faster, would make it less detailed. Of course one could always use a slower scan speed to see more details, but this would lead to long waiting times. Even though a change in bias voltage should theoretically not change anything in the resulting image, it is noteworthy that there are basically no differences in the images other than some small details. It could have been the case that even though theoretically nothing should change, there are some practical circumstances which result in differences.

6.3 Planar distance between closest neighbors of graphite

The literature value [1] for the planar distance between closest neighbors of graphite is 1.42 \AA . This value is not compatible with the values from this experiment, which are $(0.7 \pm 0.1) \text{ \AA}$ for real space and $(0.7 \pm 0.2) \text{ \AA}$ for reciprocal space. As we did not measure the data used to obtain those values ourselves, but rather got it from our tutor, it is hard to tell what went wrong. To experimentally obtain the literature value, the atoms in Fig. 11 would have to be 2.46 \AA (compare with Fig. 10) apart from each other, which they are clearly not, as also seen in Fig. 11. It is noticeable that the experimental values are almost exactly half of the literature value. This could imply that we made a mistake somewhere or the software gave the wrong scale. Again, also the piezos could have been calibrated wrongly, but it is not possible to know for sure.

7 Quellen

1. Versuchsanleitung Rastertunnelmikroskop https://wiki.physik.fu-berlin.de/fp/_media/private:ba10_anleitung_2020-01.pdf
2. Edited by James E. Mark
Physical Properties of Polymers Handbook
Second Edition ; Polymer Research Center and Department of Chemistry University of Cincinnati; Cincinnati, Ohio,
S.789 ff.
3. Quantenmechanik Skript Prof. von Oppen FU Berlin (2023): <https://www.physik.fu-berlin.de/en/einrichtungen/ag/ag-von-oppen/teaching/2023-WiSe-QM/Kapitel-3.pdf>
zuletzt zugegriffen am: 20.01.2025
4. Charles Kittel. *Einführung in die Festkörperphysik*. Oldenbourg Verlag, 2013.
5. Harry Binder. *Lexikon der chemischen Elemente*. S. Hirzel Verlag, 1999.
6. <https://de.wikipedia.org/wiki/Kohlenstoff#/media/Datei:Sp2-Orbital.svg> zuletzt zugegriffen am: 20.01.2025
7. Hans Lüth. *Solid Surfaces, Interfaces and Thin Films*. Springer Verlag, 2001.
8. J. Tersoff ' and D. R. Hamann (1985): *Theory of the scanning tunneling microscope*
9. <https://www.linearmotiontips.com/what-are-creep-drift-piezo-actuator/> zuletzt zugegriffen am: 01.02.2025
10. https://en.wikipedia.org/wiki/Hexagonal_lattice#/media/File:2d_hp.svg
last accessed 04.02.2025
11. S. Hembacher, F. J. Giessibl, J. Mannhart, and C. F. Quate, "Revealing the hidden atom in graphite by low-temperature atomic force microscopy," Proceedings of the National Academy of Sciences, vol. 100, no. 22, pp. 12 539–12 542, 2003.
https://www.researchgate.net/publication/9085590_Revealing_the_hidden_atom_in_graphite_by_low-temperature_atomic_force_microscopy
12. Åström K.J. and Hägglund T. (1995) *PID Controllers: Theory, Design and Tuning*
Instrument Society of America, P. 59 ff.
13. Li Gao (2014): *Probing Electronic Properties of Graphene on the Atomic Scale by Scanning Tunneling Microscopy and Spectroscopy*
DOI:10.2478/gpe-2014-0002